

# Overexpression, Purification, and Crystal Structure of Native ER $\alpha$ LBD

Sylvia Eiler, Monique Gangloff, Sylvie Duclaud, Dino Moras,<sup>1</sup> and Marc Ruff

Laboratoire de Biologie et Génomique Structurales 1, IGBMC, rue Laurent Fries, BP 163, 67404 Illkirch, France

Received November 10, 2000, and in revised form January 16, 2001; published online June 19, 2001

Several crystal structures of human estrogen receptor  $\alpha$  ligand-binding domain (hER $\alpha$  LBD) complexed with agonist or antagonist molecules have previously been solved. The proteins had been modified in cysteine residues (carboxymethylation) or renatured in urea to circumvent aggregation and denaturation problems. In this work, high-level protein expression and purification together with crystallization screening procedure yielded high amounts of soluble protein without renaturation or modifications steps. The native protein crystallizes in the space group P3<sub>2</sub>21 with three molecules in the asymmetric unit. The overall structure is very similar to that previously reported for the hER $\alpha$  LBD with cysteine carboxymethylated residues thus validating the modification approach. The present strategy can be adapted to other cases where the solubility and the proper folding is a difficulty. © 2001 Academic Press

**Key Words:** crystal structure; nuclear receptor; steroid; estradiol; purification; expression; crystallization.

Steroid hormones regulate the transcription of target genes in the cells by binding to transcription factors which belong to the superfamily of nuclear receptors. All the members of this family display a modular structure composed of six domains (A–F) (Fig. 1), the N-terminal A/B region harbors a ligand-independent transactivation function (AF-1), the C region forms the DNA-binding domain, and the E region constitutes the ligand-binding domain (LBD)<sup>2</sup> with a ligand-dependent

transactivation function (AF-2) (1, 2). Several crystal structures of estrogen receptor ER $\alpha$  LBD are known (3). Crystal structures have been solved in complex with estradiol (E2) (4) and the antagonists raloxifene (5) and tamoxifen (6). The human ER $\beta$  LBD has been solved in complex with genistein and raloxifene (7).

The first crystallographic investigations were hampered by the sensitivity of the protein to oxidation and aggregation. In order to cope with these problems different approaches have been used. One was to use a denaturation–renaturation process (4); the second was to modify chemically the cysteine by carboxymethylation (5). We present here the strategy used to express, purify, and crystallize ER $\alpha$  LBD in order to solve the structure in its native form without modification or renaturation. The first step to optimize the production of large amounts of soluble and functional protein in *Escherichia coli* was the choice of the cloned sequence (Fig. 1). This was based on sequence alignment analysis and structural modeling. The different constructions were tested for expression and the one that gave the largest amount of expressed protein (His<sub>6</sub>-ER(302–552)) was used for protein production optimization. Different cell culture and induction conditions were tested as well as different cell lysis and affinity chromatography buffer compositions. The purification and crystallization procedures were then refined together in order to obtain good diffracting crystals.

## MATERIALS AND METHODS

### Expression Tests

Four different constructions (Fig. 1) were inserted in the *Nde*I–*Bam*HI sites of pET15b (Novagen) (8) using

PMSF, phenylmethanesulfonyl fluoride; DTT, 1,4-dithiothreitol; EG, ethylene glycol; PEG, polyethylene glycol; CV, column volume.

<sup>1</sup> To whom correspondence should be addressed. Fax: +33-388 65 3276. E-mail: moras@igbmc.u-strasbg.fr.

<sup>2</sup> Abbreviations used: hER $\alpha$  LBD, human estrogen receptor alpha ligand binding domain; E2, estradiol; NDSB, non detergent sulfobetaine;  $\beta$ M,  $\beta$ -mercaptoethanol; DIFP, diisopropylfluorophosphonate;

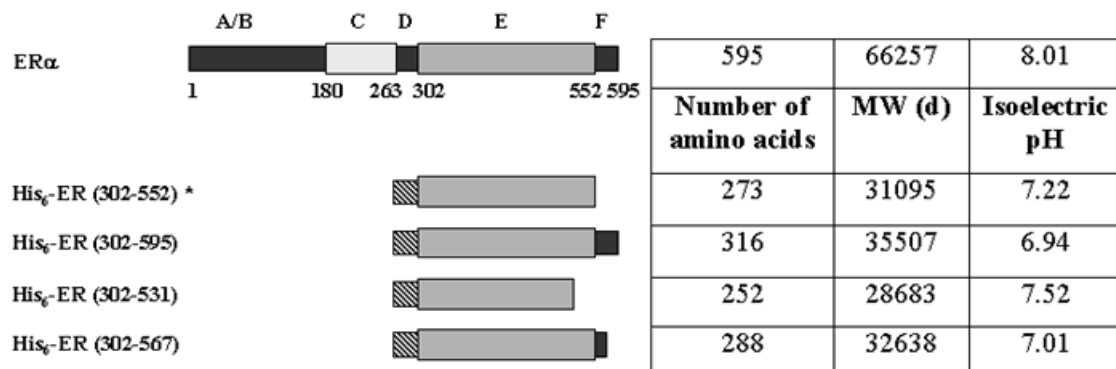


FIG. 1. Schematic representation of the modular organization of nuclear receptors and of the constructions used for expression tests with some physicochemical characteristics (molecular weight, pHi).

PCR leading to fusion proteins with a HIS-tag allowing affinity chromatography. *E. coli* BL21(DE3) cells were electroporated with 20 ng pET15b recombinant plasmid. The transformed cells were used for overnight precultures which were inoculated in 100 ml LB medium supplemented with 100  $\mu$ g/ml ampicillin and different additives were tested (10% sucrose, 10  $\mu$ M E2, 10% glycerol, 10% ethylene glycol (EG), 0.1% *n*-octyl glucoside, 10 mM 3-(1-pyridino)-1-propanesulfonate (a non-detergent sulfobetaine (NDSB)) (Fig. 2). The cells were incubated at 37°C, up to an OD<sub>600nm</sub> = 0.6. The medium temperature was then maintained at 37°C or cooled at 25 and 15°C. The expression of T7 RNA polymerase was induced with 0.5 mM isopropyl-1-thio- $\beta$ -D-galactopyranoside in the presence of 10  $\mu$ M estradiol, for 4 h at 37 or 25°C and overnight at 15°C. Cells were harvested by centrifugation and washed in 10 ml ice-cold buffers containing 50 mM Tris-HCl, pH 7.5, 50 mM NaCl, 20 mM  $\beta$ -mercaptoethanol ( $\beta$ M), and the different additives (Fig. 2). The cells were lysed by sonication with a temperature probe to keep the extract below 10°C. Diisopropylfluorophosphonate (DIFP) (0.1 mM) phenylmethanesulfonyl fluoride (PMSF) (0.1 mM), and protease inhibitor cocktail (leupeptin, pepstatin, aprotinin, antipain, and chymostatin at 1.25  $\mu$ g/ml) were added before, during, and after sonication. The extracts were centrifuged at 50,000rpm, 4°C for 1 h. The expression of soluble protein was estimated on SDS-PAGE by comparison of the amount (intensity of coloration) of ER $\alpha$  LBD in the total extract and in the centrifugation supernatant. A sketch showing this refinement procedure is presented in Fig. 2. The results of the expression optimization are shown in Fig. 3. The optimal conditions were to use the His<sub>6</sub>-hER $\alpha$  LBD(302–552) construct transformed in cells which were grown in LB medium supplemented with estradiol and sucrose. Induction was carried out for 4 h at 25°C. The cell disruption buffer contained 2 M of NDSB.

### Protein Recovery

The cell extract of the refined expression conditions was loaded on an Zn<sup>2+</sup> affinity chromatography column. The optimal concentration of NDSB, glycerol, and NaCl was determined as described in the following (Fig. 2). The imidodiacetate sites of the column were saturated with 30 column vol (CV) of 0.1 M ZnCl<sub>2</sub>, pH 4.5. Metal excess was removed by a 10 CV wash in 0.5 M NaCl. The column was equilibrated in 10 CV starting buffer (100 mM Na/K phosphate, pH 7.5, 10  $\mu$ M estradiol, 20 mM  $\beta$ -mercaptoethanol, and the different additives tested (Fig. 2)). The His<sub>6</sub>-ER $\alpha$  LBD was loaded on the column. Nonspecific binding was removed by a 10 CV wash in the starting buffer. Elution was performed in a 15 CV imidazole gradient from 0 up to 0.5M. The amount of protein was determined by the Bradford assay. The protein was then concentrated on Centricon 10 and analyzed on SDS-PAGE. The chosen affinity buffer (0.5 M NDSB, 50 mM NaCl) was the one which allowed recovery of the highest amount of protein after concentration.

### Purification

The first purification protocol was to use a gel filtration column after the affinity chromatography. The protein obtained showed one band on SDS-PAGE and a continuous smear on native gels. This protein led to bad quality crystals. A second purification procedure has been set up by adding an ion-exchange chromatography after the affinity column followed by a gel filtration. The ion-exchange column separated the protein into two peaks. On native gel the two peaks showed discrete bands, one for the first peak, and three for the second (Fig. 4). However, the protein from both peaks gave good quality crystals. The final purification procedure used is described in the following. The pellet of a 2 liters cell culture under optimized conditions was sonicated in 100 ml buffer (2 M NDSB, 50 mM NaCl, 100 mM Na/K phosphate, pH 7.5, 10  $\mu$ M estradiol, and

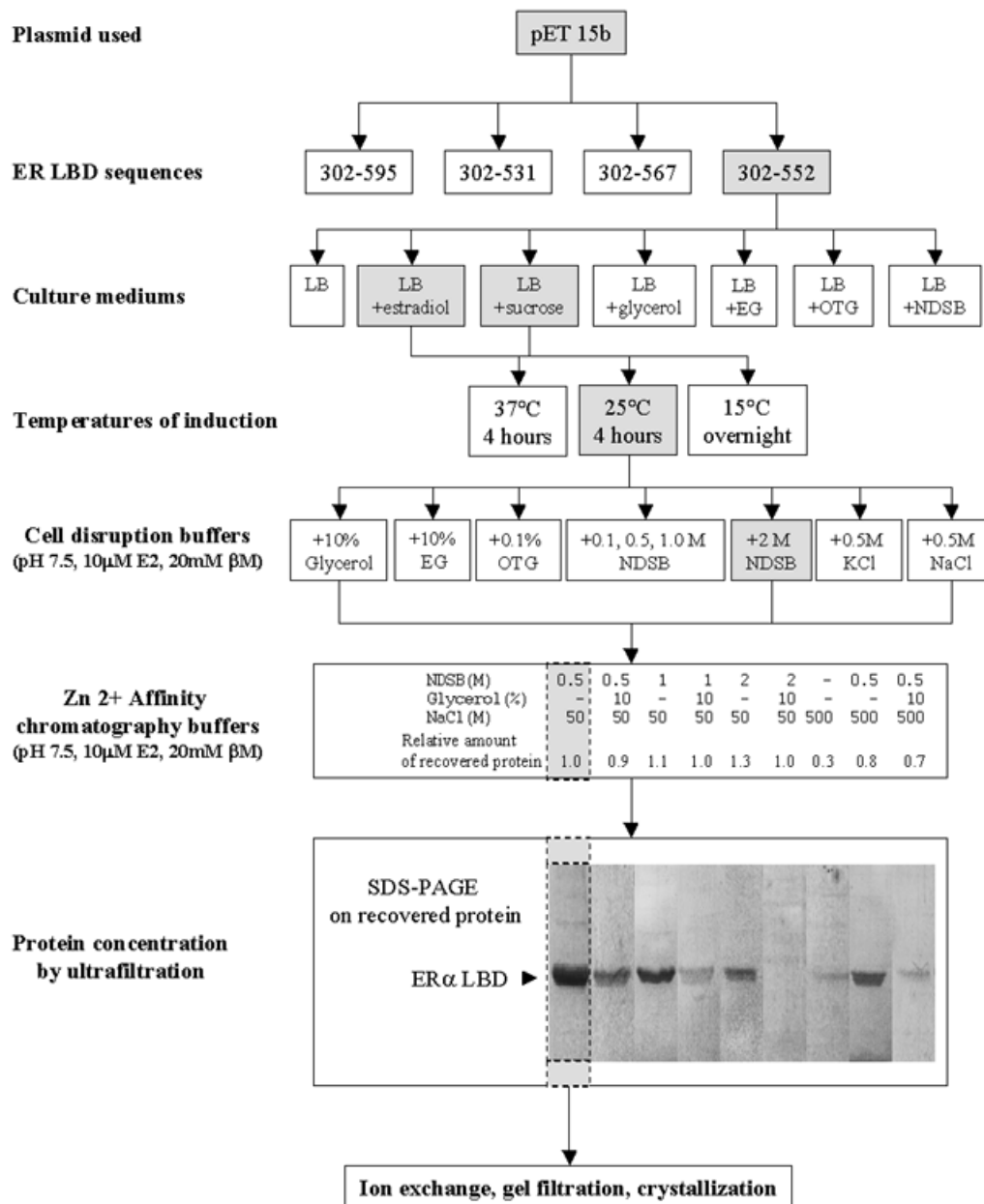


FIG. 2. Sketch summarizing the refinement procedure of protein production. The optimal conditions at each step are highlighted in gray: the His<sub>6</sub>-ER $\alpha$  LBD(302–552) construct was chosen, the bacterial culture medium was supplemented with estradiol and sucrose, followed by a 4-h induction at 25°C, and the cell disruption was done in presence of 2 M NDSB. The affinity chromatography buffer giving the highest amount of protein after concentration was 0.5 M NDSB and 50 mM NaCl as seen on SDS-PAGE.

20 mM  $\beta$ -mercaptoethanol). DIFP (0.1 mM), PMSF (0.1 mM), and protease inhibitor cocktail (leupeptin, pepstatin, aprotinin, antipain, and chymostatin at 1.25  $\mu$ g/ml) were added before, during, and after sonication. The extract was centrifuged at 50,000 rpm, 4°C for 1 h in a Beckman R60Ti rotor. The supernatant was then diluted in order to decrease NDSB concentration (0.5 M NDSB, 50 mM NaCl, 100 mM Na/K phosphate, pH 7.4, 10  $\mu$ M estradiol, 20 mM  $\beta$ -mercaptoethanol). This

extract was then loaded on a Zn<sup>2+</sup>-affinity chromatography (Poros MC, 20.1 ml bed volume) equilibrated in 10 CV starting buffer (0.5 M NDSB, 50 mM NaCl, 100 mM Na/K phosphate, pH 7.4, 10  $\mu$ M estradiol, 20 mM  $\beta$ -mercaptoethanol) at 30 ml/min. Nonspecific binding was removed by a 10 CV wash in the starting buffer. Elution was performed in a 15 CV imidazole gradient from 0 to 0.5 M. Fractions of interest were pooled and diluted in order to decrease salt concentration at 10 mM

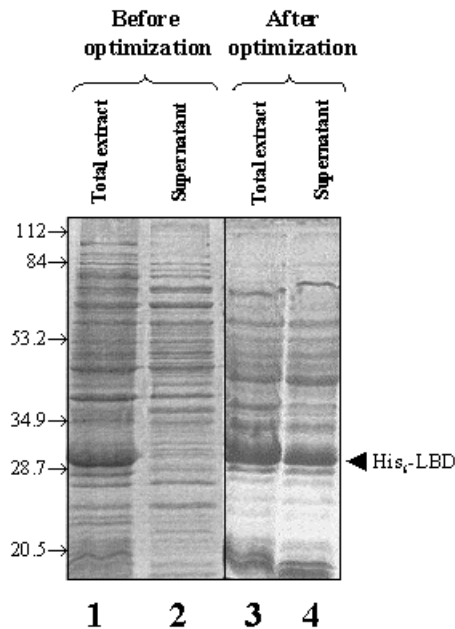


FIG. 3. Coomassie blue-stained 12% SDS-PAGE of His<sub>6</sub>-ER $\alpha$  LBD expression assays. Molecular weights of protein size markers are indicated on the left side in kDa. Lanes 1 and 2 represent, respectively, the total cell extract and supernatant obtained before optimization under standard cell culture conditions (LB medium, induction at 37°C) with a standard lysis buffer (150 mM NaCl, 50 mM Tris-HCl, pH 8): all the protein remains in the pellet. Lanes 3 and 4 represent, respectively, the total cell extract and supernatant obtained after optimization of the cell culture conditions (10% sucrose + estradiol, induction at 25°C) and the lysis buffer composition (2 M NDSB, 50 mM NaCl, 50 mM Na/K phosphate, pH 7.4, 20 mM  $\beta$ M). Most of the insoluble protein in standard conditions became soluble under the optimized conditions.

for the second purification step which was an anion-exchange chromatography on Poros HQ (1.7 ml bed volume). The column was equilibrated in 10 CV starting buffer (10 mM NaCl, 10 mM Tris-HCl, pH 8, 10  $\mu$ M estradiol, 50 mM  $\beta$ -mercaptoethanol). The diluted zinc pool was loaded on the column at 5 ml/min. A salt gradient from 10 mM to 2 M NaCl over 100 CV was used for elution. Fractions were analyzed on SDS and native PAGE and separated into two different pools which were processed separately. The protein was concentrated to 2–3 ml on Amicon YM-10 before gel filtration on a 120-ml Fractogel EMD BioSec (S) (Merck). The column was equilibrated with the following buffer: 50 mM NaCl, 50 mM Tris-maleate, pH 8, 10  $\mu$ M estradiol, 50 mM  $\beta$ -mercaptoethanol. Peak fractions with an apparent molecular weight of a dimer were pooled and concentrated by ultrafiltration (Centricon-10) to 10 mg/ml for crystallization trials. Protein concentration was determined by the Bradford assay. With this procedure we obtained 7 mg of pure protein for 2 liters of culture. Both peaks obtained after ion exchange were used for crystallization assays.

### Functional Characterization

Functional characterization of the protein was done by measuring its estradiol binding ability. Crude extracts of recombinant *E. coli* BL21(DE3)-expressing His<sub>6</sub>-ER $\alpha$  LBD were used for ligand binding assay. The concentration of His<sub>6</sub>-ER $\alpha$  LBD was determined by incubating increasing amounts of crude extract with 10<sup>-8</sup> M 40 Ci/mmol [6,7-<sup>3</sup>H(N)]-estradiol (NEN, Du Pont De Nemours) for 5 h at 4°C in the absence (for total binding) and in presence of 1000-fold excess of nonlabeled estradiol (for nonspecific binding). Bound (B) and free (F) ligands were separated by dextran-coated charcoal (9) (4% Norit A charcoal, 0.4% dextran T-70 in the binding buffer: 1 M NDSB, 50 mM NaCl, 50 mM Tris-HCl pH 8, 1 mM EDTA, 1 mM DTT). This mixture was left on ice for 5 min and centrifuged at 12,000*g* for 5 min. The supernatant was removed for scintillation counting. Each measure was performed in triplicate. For Scatchard analysis, the protein was incubated with increasing concentrations of radiolabeled estradiol (from 10<sup>-10</sup> to 10<sup>-7</sup> M) for 20 h at 4°C. The samples were processed as described before. The change of B/F as a function of F was analyzed by a least square fitting method which determines the dissociation constant  $K_d$ , the receptor concentration  $B_{max}$ , and the nonspecific binding rate (10). The dissociation constant for the recombinant molecule ( $K_d = 0.26$  nM) is in agreement with the previous published results (11).

### Crystallization

Crystallization trials were carried out at two different temperatures (4 and 24°C) by varying the geometry of the system, screening various precipitating agents and additives, and using salting-in and salting-out methods. Hanging drops were performed on siliconized coverslips in Linbro plate and sitting drops using Cryschem Hampton plates (final drop volume 1–10  $\mu$ l). For microbatch technique we used the IMPAX crystallization robot (final drop volume 1–4  $\mu$ l), the mixture was dropped on a NUNC HLA 72  $\times$  10 plate filled previously with decane. Dialysis assays were done using the Zeppezauer technique (12). For crystallization in gel we used the Hampton silica hydrogel in capillaries. The refinement of crystallization conditions was mostly done with the hanging drop technique. For the screening of precipitating agent, additives, speed of equilibration, and protein concentration, we mixed protein solution to reservoir solution and/or additives with different ratio of precipitating agent concentration between reservoir and drop. This was performed using the Hampton sparse matrix solutions and/or more specific additives (imidazole, NDSB, detergents). Diffracting crystals were obtained in droplets of 2 to 8  $\mu$ l containing 5 mg/ml of protein (in 50 mM NaCl, 50 mM

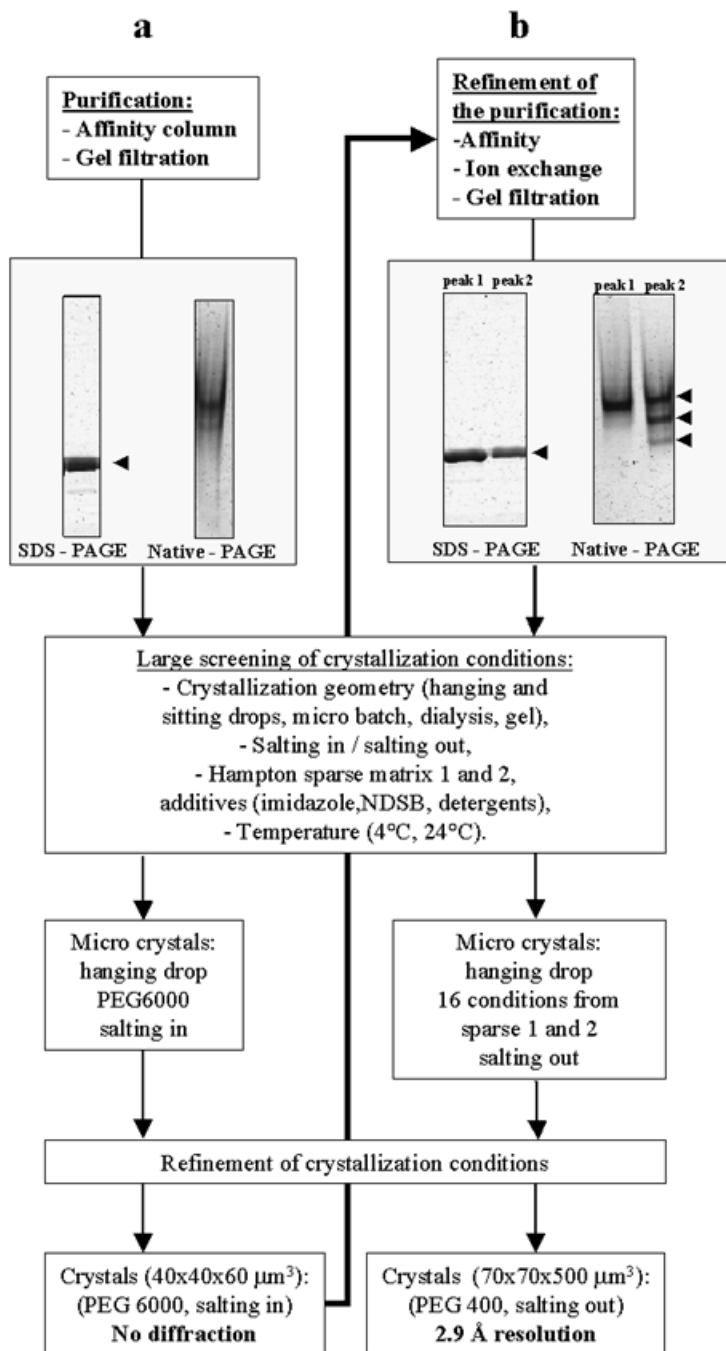


FIG. 4. Refinement of the purification and the crystallization procedure. (a) The procedure after an affinity and a gel filtration chromatography purification. A Coomassie blue-stained 12% SDS-PAGE and 6% native PAGE are shown. Despite the fact that the SDS-PAGE shows a unique band indicating a pure protein, the native PAGE shows a continuous smear reflecting an heterogeneity. This procedure led to bad quality crystals. An ion-exchange chromatography was then added to the purification protocol shown in (b). The anion-exchange permitted the separation of two protein populations (peak 1 and peak 2). The SDS-PAGE shows a unique band for both peaks while the native PAGE shows one band for peak 1 and three discrete bands for peak 2 indicating a reduced heterogeneity compared to (a). However, the protein from both peaks led to good diffracting crystals.

Tris-maleate/HCl, pH 8, 10  $\mu\text{M}$  estradiol, 50 mM  $\beta$ -mercaptoethanol), 2 to 10% polyethylene glycol (PEG) 400, 150 to 400 mM NaCl, 50 mM  $\beta$ -mercaptoethanol, and 50 mM imidazole at various pH around pH 7.3.

Droplets were equilibrated at 4°C against a 500  $\mu\text{l}$  reservoir of 4 to 20% PEG400, 350 to 950 mM NaCl, 50 mM imidazole at the same pH that the droplet, and 50 mM  $\beta$ -mercaptoethanol in order to concentrate the

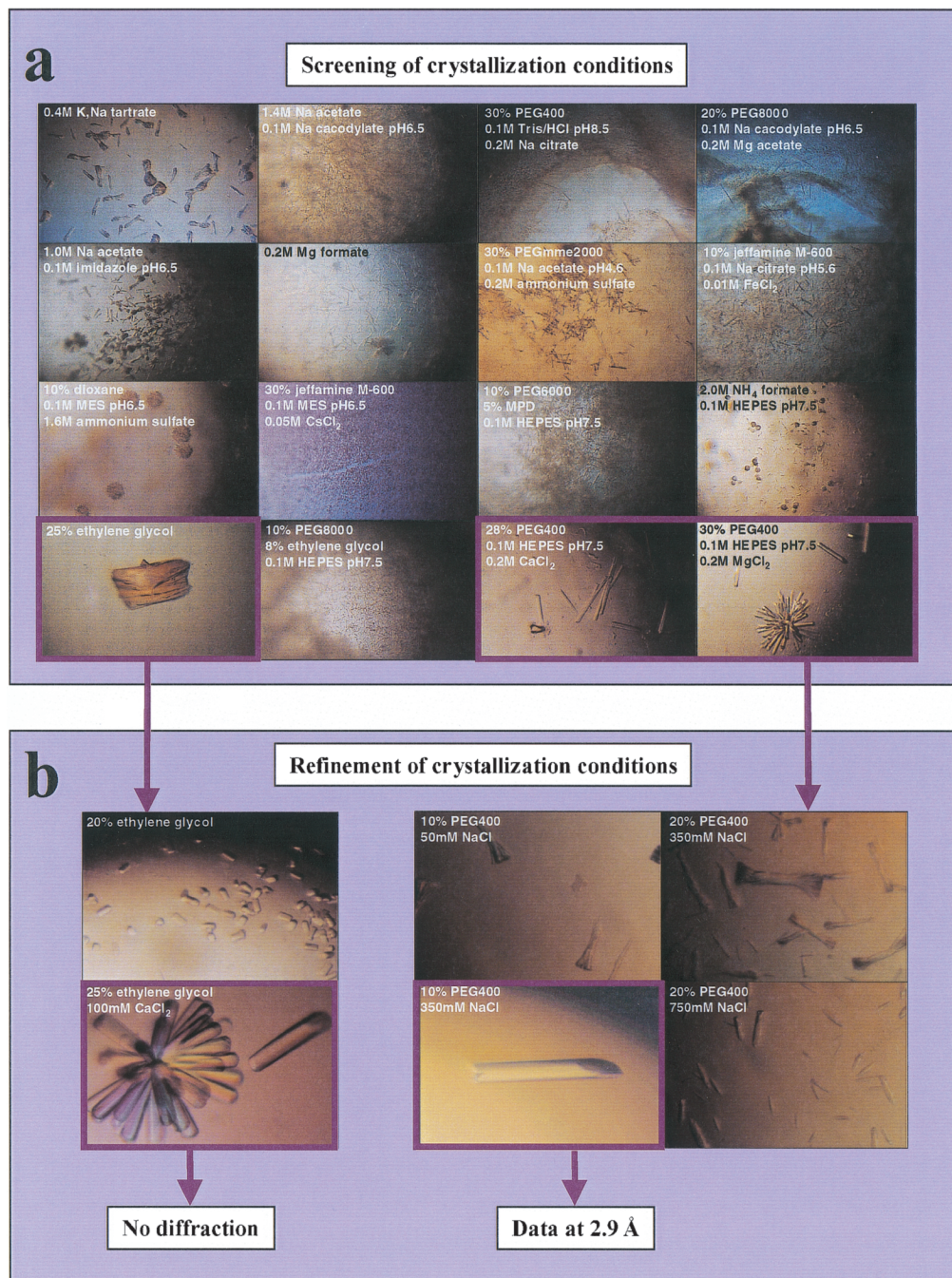


FIG. 5. (a) The conditions which gave microcrystals after a large screening on the protein obtained after affinity, ion-exchange, and gel filtration chromatography are presented. The conditions giving the largest microcrystals have been refined for crystal growth (EG, PEG400). (b) Refinement of conditions using ethylene glycol as precipitating agent led to crystals without diffraction capacity. The refinement of crystallization conditions using PEG400 as precipitating agent led to crystals diffracting up to 2.9 Å resolution. The crystal growth was very sensitive to the PEG/NaCl ratio.

droplet twice. The ratio PEG/NaCl was critical for crystal growth and was screened for each protein preparation (Fig. 5). About 5 weeks was necessary for these crystals (350 mM NaCl, 10% PEG400) to achieve their final size of about  $70 \times 70 \times 500 \mu\text{m}^3$ .

#### *Protein Characterization in Crystals*

In order to analyze the crystal content, they were washed in mother liquor and dissolved in water. The protein was analyzed on SDS-PAGE and transferred

to a nitrocellulose membrane for a Western blot analysis. The primary rabbit antibody (1:10,000) was raised against the hexahistidine-tag; the second antibody was a goat anti-rabbit IgG (1:10,000) linked to horseradish peroxidase. Enhanced chemiluminescence reagents were added for detection (Amersham Pharmacia Biotech). N-terminal sequencing was performed on protein transferred to PVDF membrane using the Edman technique. The SDS gel, Western blot, and sequencing confirmed the presence of a full-length ER $\alpha$  LBD plus the His-tag peptide in the crystals.

### Structure Determination

The wild-type ER $\alpha$ LBD crystallizes in the trigonal space group P3(2)21. Crystals were transferred in mother liquor containing a cryoprotectant agent before being flash-cooled in liquid ethane and stored in liquid nitrogen. The cryoprotectant used was 6% PEG400, 25% ethylene glycol for crystals grown at low PEG amounts or 30% PEG400 for crystals obtained in presence of 20% PEG400. X-ray data were collected at 120°K in a nitrogen gas stream using synchrotron radiation (ESRF, LURE). Data were integrated and reduced using the programs DENZO and SCALEPACK (13). Initial phases were obtained with AMORE (14) using a mutant (Cys  $\rightarrow$  Ser) monomer structure (15) as a search model. The correct solution corresponding to one dimer and a monomer of ER $\alpha$  LBD in the asymmetric unit had a correlation coefficient of 45.6% and a *R*-factor of 40.8% after AMORE rigid body refinement. Refinement was performed with CNS (16) using bulk solvent corrections and non crystallographic restraints. All data between 30 and 2.9 Å resolution were included with no sigma cutoff (Table 1).

## RESULTS AND DISCUSSION

The structure exhibits the predominantly  $\alpha$  helical fold observed for other nuclear receptor structures (Fig. 6a). The asymmetric unit contains three monomers: one of them forms a dimer through the crystallographic two fold, and the two other form the noncrystallographic dimer. The superposition of the three monomers led to an rmsd of 0.2 Å over 235 C $\alpha$ -atoms. H12 is lying in the "agonist position" (4) and the antagonist cleft is filled by packing contacts with the loop H3–H4 from another molecule. The superposition with antagonist structures or in complex with a coactivator peptide (GRIP1) (6) shows that the packing contact is similar to the coactivator–receptor contact or H12–receptor contact (Fig. 6b). To prevent aggregation of LBDs we suggest that residue Leu372 could be mutated in some more hydrophilic residue like a serine. The comparison of this structure with the carboxymethylated one (6) showed no significant differences (rmsd of 0.38 Å over

**TABLE 1**  
Data Processing, Phase Determination, and Refinement Statistics (P3<sub>2</sub>21,  $a = b = 105.5$  Å,  $c = 136.08$  Å,  $\alpha = \beta = 90^\circ$ ,  $\gamma = 120^\circ$ )

Data Processing	
Space group	P3 <sub>2</sub> 21
Resolution (Å)	2.9
Unique reflections	18142
Completeness (%) <sup>a</sup>	91.0 (78.0)
Multiplicity	1.8
<i>R</i> <sub>sym</sub> (%)	8.0
Refinement (three molecules per asymmetric unit)	
Resolution (Å)	15–2.9
Number of reflections in working set	16364
Number of reflections in test set	1778
Number of protein atoms	5886
Number of heterogen atoms	60
Number of water molecules	165
Working <i>R</i> factor (%)	24.1
Free <i>R</i> factor (%)	31.0
Rmsd bond lengths (Å)	0.014
Rmsd bond angles (deg)	1.5
Average <i>B</i> -factor (Å <sup>2</sup> )	61.2
Protein	62.1
Ligand	35.6
Water	40.8

Note:  $R_{sym} = \frac{\sum_h \sum_i |I(h) - \langle I(h) \rangle|}{\sum_h \sum_i I(h)}$ , where  $\langle I(h) \rangle$  is the average intensity of reflection  $h$ ,  $\sum_h$  is the sum over all reflections, and  $\sum_i$  is the sum of all measurements of reflection  $h$ .

<sup>a</sup> The value in parentheses corresponds to the last shell of resolution (3.1–2.9 Å)

235 C $\alpha$ -atoms). In particular the position of hydrophobic residues lining the ligand binding pocket are highly conserved with a rmsd of 0.2 Å. Despite these similarities, the side chains of Arg394 and Glu353 which anchors the estradiol in the ligand pocket have a slight shift of 1 Å that does not affect the estradiol positioning. All these results show that carboxymethylation does not affect the structure of the ER $\alpha$  LBD.

The different steps for the production of large amounts of stable and pure protein (sequence limits of the expressed domain, overexpression conditions of functional protein, cell disruption, purification) have been optimized. These steps are summarized in Fig. 2. For protein expression the cells were grown in presence of estradiol and sucrose, the induction was done at 25°C. The need of estradiol for expression and purification could be explained by the fact that ER $\alpha$  LBD is unstable without ligand. The addition of sucrose is thought to change the medium viscosity and slow down the protein synthesis after induction allowing a proper folding. It has been used successfully to increase the amount of soluble protein in several cases (17, 18). Lowering the induction temperature has the same effect. Among the

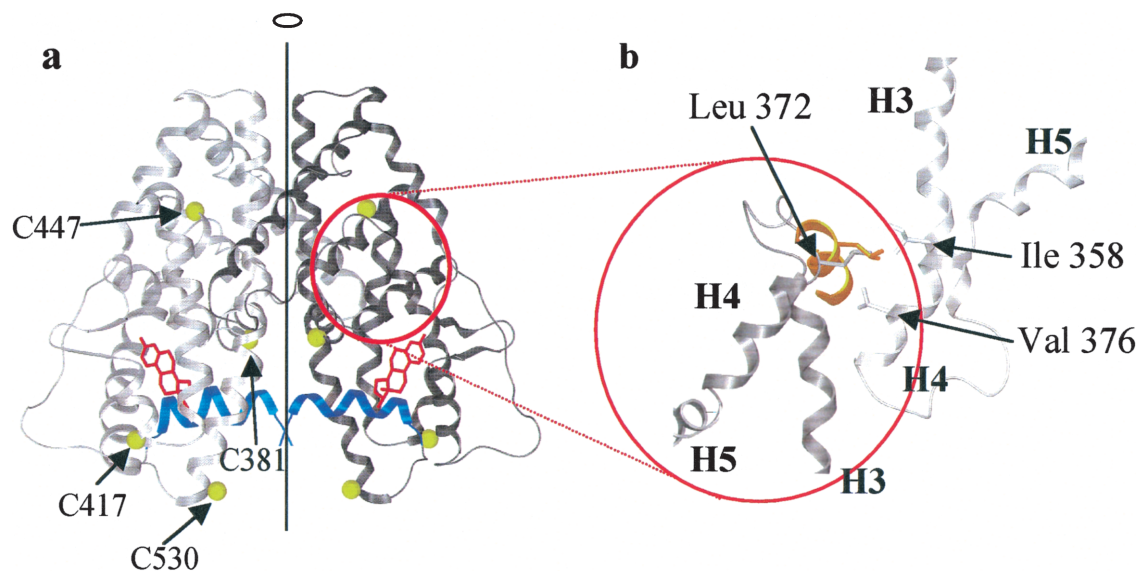


FIG. 6. (a) 3D structure of the wild-type ER $\alpha$  LBD dimer. One monomer is shown in gray, and the other one in black. The activation helix H12 (blue) is in the agonist position. Estradiol is shown in red and the position of the four cysteines is shown as yellow dots. (b) Close-up view on the loop between helix 3 and 4 (in dark gray), making packing contacts with a symmetry related molecule (in light gray) in the coactivator binding groove. This molecule has been superposed on the structure of the complex with a peptide from a coactivator protein. The interaction of Leu372 is similar to that observed with the coactivator peptide (shown in gold).

different additives tested for the cell disruption buffer, the highest amount of protein was obtained using 2 M NDSB while the buffer used for the affinity chromatography contained 0.5 M NDSB, which had the best yield in protein recovery after concentration. NDSB has a solubilizing effect (19) which is different in the purified protein solution compared to the crude extract probably due to the presence of contaminant proteins lowering its effective concentration in solution. High amounts of reducing agent like  $\beta$ -mercaptoethanol were added at each step of the procedure to prevent oxidation of the accessible cysteines. The purification procedure was optimized by the addition of an ion-exchange column before the gel filtration (Fig. 4). This ion-exchange column separated the protein into two peaks, similar on SDS-PAGE, but different on native PAGE (one band for peak 1 and three bands for peak 2). When submitted to a gel filtration column each peak elutes with the apparent molecular weight of a dimer. These heterogeneity arose certainly from adsorbed NDSB molecules on the protein surface as suggested by mass spectrometry experiment (data not shown).

The crystallization screening was done on protein issued from the purification with and without ion exchange. After the first purification, microcrystals have been obtained in PEG6000 and the crystallization conditions have been refined. These crystals obtained in salting in conditions did not diffract. After the addition of an anion-exchange column, microcrystals appeared in various conditions from the Hampton screen I and II for the two peaks. Each of these hits were then refined

(carboxylic acids such as tartrate, acetate, formate, non-volatile polyalcohols of different size (EG, methylpentane diol, PEG)). Most of them stayed as microcrystals. Two conditions gave crystals of reasonable size and were then refined (EG and PEG400) (Fig. 5). Crystals obtained in EG had no diffracting capacity whereas crystals obtained in PEG400 diffracted up to 2.9 Å resolution. Interestingly protein from peaks 1 and 2 gave good quality crystals suitable for X-ray analysis while protein obtained without ion exchange did not. It shows that the heterogeneity of protein from peak 2 seen in native gels does not influence the quality of crystals, thus raising a question about the effect of the anion exchange on crystallization. It could be that this purification removes part of the heterogeneity (smear  $\rightarrow$  discrete bands on native gel) due to small charged molecules (NDSB).

## CONCLUSION

In this work we were able to set up a strategy that allowed us to optimize the procedure for protein expression, purification, and crystallization, leading to the production of large amounts of soluble and functional protein as well as reproducible hER $\alpha$  LBD X-ray suitable crystals. The different steps in this procedure are the following: (i) for the expression several protein sequences were used and then the composition of the culture medium, the temperature, and duration of induction were varied; (ii) for the protein recovery we investigated various buffer composition for cell lysis

and affinity chromatography; and (iii) the crystallization process was refined together with the purification protocol. The rationalization of the protein expression and purification (Figs. 1–3) together with the crystallization screening procedure (Figs. 4 and 5) yielded large quantities of protein that allowed us a successful study by X-ray crystallography (Fig. 6).

#### ACKNOWLEDGMENTS

We thank A. Litt and A. Mitschler for helpful contribution to data collection; N. Potier for mass spectrometry measurements; J. M. Garnier for cloning; the peptide and DNA sequencing and synthesis services of IGBMC for their availability; and the staff of ESRF, LURE, and DESY for their help during data collection. This work was supported by funds from Schering AG, CNRS, and grants from the Ministère de la Recherche et de l'Enseignement Supérieur and the Association pour la Recherche sur le Cancer. The coordinates have been deposited at the PDB with the Accession No. 1G50.

#### REFERENCES

- Mangelsdorf, D. J., and Evans, R. M. (1995) The RXR heterodimers and orphan receptors. *Cell* 83, 841–850.
- Katzenellenbogen, J. A., and Katzenellenbogen, B. S. (1996) Nuclear hormone receptors: ligand-activated regulators of transcription and diverse cell responses. *Chem. Biol.* 3, 529–536.
- Ruff, M., Gangloff, M., Wurtz, J. M., and Moras, D. (2000) Structure–function relationship in DNA- and ligand-binding domains of estrogen receptors. *Breast Cancer Res.* 2, 353–359.
- Tanenbaum, D. M., Wang, Y., Williams, S. P., and Sigler, P. B. (1998) Crystallographic comparison of the estrogen and progesterone receptor's ligand binding domains. *Proc. Natl. Acad. Sci. USA* 95, 5998–6003.
- Brzozowski, A. M., Pike, A. C., Dauter, Z., Hubbard, R. E., Bonn, T., Engstrom, O., Ohman, L., Greene, G. L., Gustafsson, J. A., and Carlquist, M. (1997) Molecular basis of agonism and antagonism in the oestrogen receptor. *Nature* 389, 753–758.
- Shiau, A. K., Barstad, D., Loria, P. M., Cheng, L., Kushner, P. J., Agard, D. A., and Greene, G. L. (1998) The structural basis of estrogen receptor/coactivator recognition and the antagonism of this interaction by tamoxifen. *Cell* 95, 927–937.
- Pike, A. C., Brzozowski, A. M., Hubbard, R. E., Bonn, T., Thorsell, A. G., Engstrom, O., Ljunggren, J., Gustafsson, J. A., and Carlquist, M. (1999) Structure of the ligand-binding domain of oestrogen receptor beta in the presence of a partial agonist and a full antagonist. *EMBO J.* 18, 4608–4618.
- Studier, F. W., and Moffatt, B. A. (1986) Use of bacteriophage T7 RNA polymerase to direct selective high-level expression of cloned genes. *J. Mol. Biol.* 189, 113–130.
- Rafestin-Oblin, M. E., Couette, B., Radanyi, C., Lombes, M., and Baulieu, E. E. (1989) Mineralocorticosteroid receptor of the chick intestine: Oligomeric structure and transformation. *J. Biol. Chem.* 264, 9304–9309.
- Claire, M., Rafestin-Oblin, M. E., Michaud, A., Corvol, P., Venot, A., Roth-Meyer, C., Boisvieux, J. F., and Mallet, A. (1978) Statistical test of models and computerised parameter estimation for aldosterone binding in rat kidney. *FEBS Lett.* 88, 295–299.
- Anstead, G. M., Carlson, K. E., and Katzenellenbogen, J. A. (1997) The estradiol pharmacophore: Ligand structure–estrogen receptor binding affinity relationships and a model for the receptor binding site. *Steroids* 62, 268–303.
- Zeppenzauer, M. (1971) Formation of large crystals. *Methods Enzymol.* 22, 253–266.
- Otwinowski, Z., and Minor, W. (1997) Processing X-ray diffraction data collected in oscillation mode. *Methods Enzymol.* 276, 307–326.
- Navaza, J. (1994) Amore: An automated package for molecular replacement. *Acta Crystallogr. A* 50, 157–163.
- Gangloff, M., Ruff, M., Eiler, S., Duclaud, S., Wurtz, J. M., and Moras, D. (2001) Crystal structure of a mutant hER $\alpha$  ligand-binding domain reveals key structural features for the mechanism of partial agonism. *J. Biol. Chem.* 276, 15059–15065.
- Brünger, A. T., Adams, P. D., Clore, G. M., Delano, W. L., Gros, P., Grosse-Kunstleve, R. W., Jiang, J. S., Kuszewski, J., Nilges, M., Pannu, N. S., Read, R. J., Rice, M. L., Simonson, T., and Warren, G. L. (1998) Crystallography & NMR system: A new software suite for macromolecular structure determination. *Acta Crystallogr. D* 54, 905–921.
- Sawyer, J. R., Schlom, J., and Kashmiri, S. V. (1994) The effects of induction conditions on production of a soluble anti-tumor sFv in *Escherichia coli*. *Protein Eng.* 7, 1401–1406.
- Kipriyanov, S. M., Moldenhauer, G., and Little, M. (1997) High level production of soluble single chain antibodies in small-scale *Escherichia coli* cultures. *J. Immunol. Methods* 200, 69–77.
- Vuillard, L., Braun-Breton, C., and Rabilloud, T. (1995) Non-detergent sulphobetaines: a new class of mild solubilization agents for protein purification. *Biochem. J.* 305(Pt. 1), 337–343.